

Design and Implementation of Disturbance Observer Based Enhanced Robust Finite Control Set Predictive Torque Control for Induction Motor Systems

Abstract—To control an induction motor by directly using natural switching characters, finite control set based predictive torque control (PTC) method is studied, the optimized switching vector is selected to minimize the error between reference electromagnetic torque, stator flux signals and predicted values in the cost function. Similar to direct torque control (DTC) method, PTC method does not need a modulator and an internal current PI controller, it has fast torque response, but the variable prediction of traditional PTC method is depended on system model which exists the problem of parameter uncertainties. In addition, the torque reference in the cost function is generated by PI speed controller which is a slow manner, the torque reference generating rate and accuracy is not good especially when the load torque and inertial value are variation. This paper investigates a disturbance observer (DOB) based predictive torque control (PTC) approach for induction motor systems subject to load torque disturbance, parameter uncertainty and time delay. Not only speed loop adopts DOB based feedforward compensation method for improving the system disturbance reject ability and robustness, the flux, current and torque prediction are also compensated and improved by using this technique. The simulation and experimental results verified the effectiveness of the proposed method.

Index Terms—induction motor, disturbance observer (DOB), predictive torque control (PTC), direct torque control (DTC), robustness, disturbance reject ability.

I. INTRODUCTION

Direct torque control (DTC) method are widely applied for AC machines due to the fast transient torque response, easy to be implemented which has no modulator and internal current PI controller [1]-[7]. However, because of the hysteresis characteristic of DTC, conventional DTC has two drawbacks. First, the switching frequency is variable and dependent on the hysteresis bands. Second, the torque ripple are considerable [3]-[5]. In recent years, considering the natural character of inverter, the so called finite control set model predictive control (FCS-MPC) is proposed, many researchers arouse more attention on applications of FCS-MPC where it contributes with several advantages such as fast transient response, simple implementation and straightforward handling of nonlinearities and constraints.

Finite control set model predictive control is also a branch of model-based predictive control method which is an advanced control scheme in industry system. Different from continuous model predictive control for controlling AC motors, continuous MPC methods need a modulator in the motor system design. However, FCS-MPC methods incorporate the inverter model directly into the controller, all feasible inverter switching states are considered in order to minimize the cost function. The cost function of FCS-MPC is very flexible, predictive torque control (PTC) also belongs to the family of FCS-MPC method which includes the errors of between the torque reference and estimated (predicted) value and other terms such as over-current protection, and

so on [8]-[11]. It is a considerable alternative to DTC for AC motors and has also been verified in many existed results [8]-[16].

It is well known that induction motor system model is nonlinear and strong coupled, in addition, the system parameters uncertainty and load disturbance unknown are also inevitable [17]-[25]. Although the PTC control method is a nonlinear control method in nature, but the direct use of system models for selecting the optimal control actions make predictive methods prone to changes in their performance when facing modeling errors of parameter variations and load torque unknown. There are some works have been done on the robustness issue of predictive control application [19]-[22]. The paper [19] proposes an adaptive parameter identification technique for ac-dc active front ends to overcome model mismatch and parameter uncertainty. The model reference adaptive control and sliding mode control method have been proposed for the same issue in [12]-[14]. Other studies have focused on the influence of resistance and inductance uncertainties on the prediction model of FCS-MPC [20]-[22]. These works concluded that the influence of parameter uncertain and load disturbance in the prediction model remains as an important concern.

Recently, due to the undesirable influences of external disturbances and model parameter uncertainties, the researchers have raised an increasing deal of interest on disturbance estimation based feedforward compensation methods [26]-[35]. Extended state observer (ESO) is a kind of disturbance estimate technique which regards the lumped disturbances as a new state of system [27]. It can observe both system states and disturbances, then the observed value of disturbances can be employed to compensate in the feedforward channel to improve the performance of system, such as in PMSM servo systems [28]-[29], DC-DC converter system [32]. Disturbance observer based control (DOBC) has been proved to be effective to reduce the effects of unknown external disturbances and model uncertainties by compensating it from the feedforward channel [30], [31], [34], such as in two-link robotic manipulator systems [34], and so on. The major advantage of the DOBC is that the disturbance rejection ability of closed-loop system is improved without sacrificing its nominal control performance [31].

In this paper, analysis the natural characters of induction motor systems and aiming to improve the system performance with torque load disturbances and system parameter variation, disturbance observer (DOB) based finite control set predictive torque control method is developed to completely counteract the disturbance/uncertainty for induction motor system. For the cost function of PTC method, the torque reference is very important. Based on the disturbance estimation technique, the torque reference can be generated faster and more precise, especially when the load torque is given and the inertia is varying.

In addition, the parameter uncertainty also influences the estimation accuracy of stator current and flux, the disturbance observer technique is also adopted. At the end, a better convergence performance and a stronger robust ability against load disturbances and parameter variation are achieved with the proposed control scheme, which is shown by simulation and experimental results.

This paper is organized as follows. Section II gives the induction motor system and two level inverter model description. The disturbance estimation and the finite control set predictive torque controller are designed in Section III. In Section IV, numerical simulation and experimental results will show the effectiveness of the proposed controller. Then a conclusion ends the paper.

II. MODEL DESCRIPTION OF INDUCTION MOTOR AND INVERTER

A squirrel-cage IM can be described by a set of nonlinear equations using a stator reference frame as follows.

$$v_s = R_s \cdot i_s + \frac{d}{dt} \psi_s \quad (1)$$

$$0 = R_r \cdot i_r + \frac{d}{dt} \psi_r - j \cdot \omega_e \cdot \psi_r \quad (2)$$

$$\psi_s = L_s \cdot i_s + L_m \cdot i_r \quad (3)$$

$$\psi_r = L_r \cdot i_r + L_m \cdot i_s \quad (4)$$

$$\frac{d\omega}{dt} = \frac{T_e}{J} - \frac{T_L}{J} - \frac{B\omega}{J} \quad (5)$$

$$T_e = \frac{3}{2} \cdot p \cdot \text{Im}(\psi_s^* \cdot i_s) \quad (6)$$

where v_s denotes the stator voltage vector; ψ_s and ψ_r represent the stator flux and rotor flux, respectively. i_s and i_r are the stator and rotor currents, respectively. R_s and R_r are the stator and rotor resistances, respectively. L_s , L_r and L_m are stator, rotor and mutual inductances, respectively; and ω , ω_e are the mechanical and electrical speeds. p is the number of pole pairs, and T_e denotes the electromagnetic torque.

A two-level voltage source inverter and its voltage vectors are employed as Fig.1. The switching state S can be expressed by the vector as follows:

$$S = \frac{2}{3}(S_a + aS_b + a^2S_c) \quad (7)$$

where $a = e^{j2\pi/3}$, $S_i = 1$ means S_i is on and \bar{S}_i is off, and $i = a, b, c$. The voltage v_s is related to the switching state S by

$$v_s = V_{dc}S \quad (8)$$

where V_{dc} is the dc link voltage. Considering the switched nature of power converters, where only a finite number of output states is available, so the so-called finite control set model predictive control (FCS-MPC) is proposed.

III. DISTURBANCE OBSERVER BASED ENHANCED ROBUST PREDICTIVE TORQUE CONTROL DESIGN

In this paper, we focus on the disturbance observer based predictive torque control for the induction motor system. The

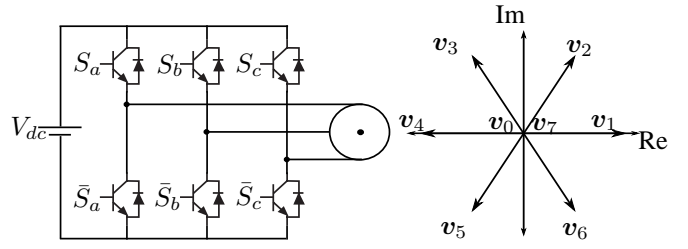


Fig. 1: Left: two-level voltage source inverter; right: voltage vectors.

control structure of induction motor systems is described as Fig. 2, the design of disturbance observer based predictive torque controller is proposed by the following three steps. First, a disturbance observer is employed to estimate the lumped disturbances. Second, stator current and flux observers are designed respectively. At the end, a novel predictive torque controller is then designed for induction motor system based on the disturbance observation.

A. Disturbance Observer

The objective of this section is to design a disturbance estimator for observing the lumped disturbances caused by torque load changes and parameter variation. On the basis of speed mathematical model (5), the speed equation can be rewritten as $\dot{\omega} = \frac{T_e^*}{J_n} + d_\omega(t)$, the lumped disturbance is denoted as $d_\omega(t) = -\frac{T_e^*}{J_n} + \frac{T_e}{J} - \frac{T_L}{J} - \frac{B\omega}{J}$. Based on the disturbance observer technique (DOB), the disturbance estimation $\hat{d}_\omega(t)$ is designed as:

$$\begin{aligned} \dot{z}_1 &= \frac{T_e^*}{J_n} + \hat{d}_\omega(t) \\ \hat{d}_\omega(t) &= \lambda_1(\omega - z_1). \end{aligned} \quad (9)$$

where the $z_1 = \hat{\omega}$ and $\lambda_1 > 0$.

Assumption 3.1: For the above induction motor system, suppose that disturbances $d(t)$ are constants in steady state, i.e., $\lim_{t \rightarrow \infty} \dot{d}_\omega(t) = 0$.

Definition 3.1: [36] A continuous function $\alpha : [0, a) \rightarrow [0, \infty)$ is said to belong to class \mathcal{K} if it is strictly increasing and $\alpha(0) = 0$. It is said to belong to class \mathcal{K}_∞ if $a = \infty$ and $\alpha(r) \rightarrow \infty$ as $r \rightarrow \infty$. A continuous function $\beta : [0, a) \times [0, \infty) \rightarrow [0, \infty)$ is said to belong to class \mathcal{KL} if, for each fixed s , the mapping $\beta(r, s)$ belongs to class \mathcal{K} with respect to r and, for each fixed r , the mapping $\beta(r, s)$ is decreasing with respect to s and $\beta(r, s) \rightarrow 0$ as $s \rightarrow \infty$. To introduce the notation of input-to-state stability (ISS), consider the system

$$\dot{x} = f(t, x, u), x \in R^n, u \in R^m. \quad (10)$$

Definition 3.2: [36] The system (10) is said to be ISS if there exist a class \mathcal{KL} function β and a class \mathcal{K} function γ such that for any initial state $x(t_0)$ and any bounded input $u(t)$, the solution $x(t)$ exists for all $t \geq t_0$ and satisfies

$$\|x(t)\| \leq \beta(\|x(t_0)\|, t - t_0) + \gamma\left(\sup_{t_0 \leq \tau \leq t} \|u(\tau)\|\right). \quad (11)$$

Such a function γ in (11) is referred to as an ISS-gain for system (10). As shown in [36], ISS implies that system (10)

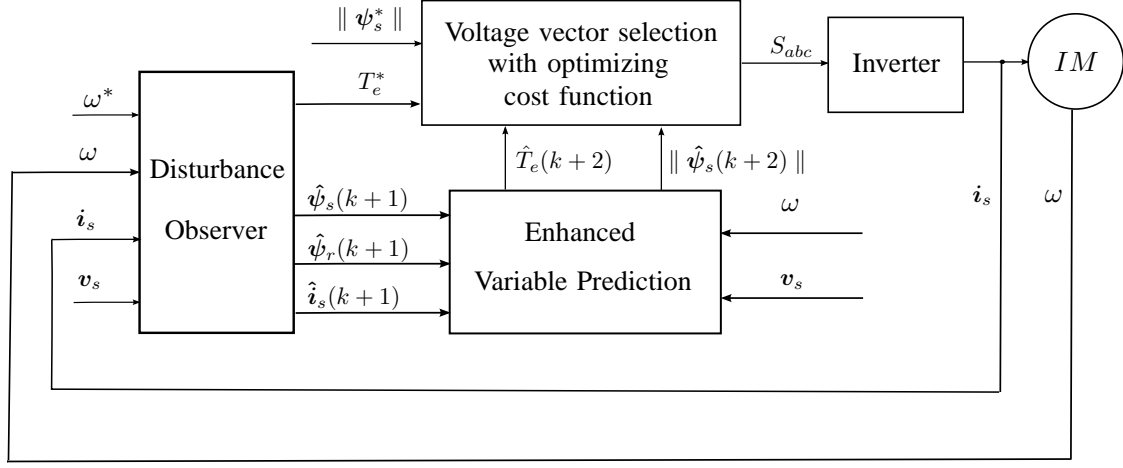


Fig. 2: Block diagram of disturbance observer based enhanced robust predictive torque control .

is bounded-input bounded-state stable when $u \neq 0$ and its zero solution (with $u = 0$) is globally asymptotically stable (GAS).

Lemma 3.1: [36] Consider a nonlinear system $\dot{x} = F(x, w)$ which is input-to-state stable (ISS). If the input satisfies $\lim_{t \rightarrow 0} w(t) = 0$, then the system states satisfy $\lim_{t \rightarrow 0} x(t) = 0$.

For the system of Eqs. (9); (DOB), define

$$e_\omega(t) = \omega - z_1 \quad (12)$$

$$e_d(t) = d_\omega(t) - \hat{d}_\omega(t) \quad (13)$$

By taking the time derivative of $e_\omega(t)$, $e_d(t)$, we obtain

$$\dot{e}_\omega(t) = e_d \quad (14)$$

$$\dot{e}_d(t) = \dot{d}_\omega - \lambda_1 e_d \quad (15)$$

The Lyapunov function is defined as follows

$$V_{e_d} = \frac{1}{2} e_d^2 \quad (16)$$

By taking the time derivative of V_{e_d} using Eqs. (14)-(15), it yields

$$\dot{V}_{e_d} = e_d \dot{e}_d \quad (17)$$

$$= e_d (\dot{d}_\omega - \lambda_1 (\dot{\omega} - \dot{z}_1)) \quad (18)$$

$$= -\lambda_1 e_d^2 + e_d \dot{d}_\omega \quad (19)$$

Suppose that the Induction motor system satisfies Assumption 3.1, then the error system of Eqs. (12)-(13) is ISS. Noting that $\lim_{t \rightarrow 0} \dot{d}_\omega(t) = 0$, from Lemma 3.1, then it can be concluded that $\lim_{t \rightarrow 0} e_d(t) = 0$, $\lim_{t \rightarrow 0} e_\omega(t) = 0$, where $\lambda_1 > 0$, the error states of Eqs. (12)-(13) will converge to the desired equilibrium point asymptotically.

B. Stator Flux and Electromagnetic Torque Observers

The PTC method is described in Fig. 2, the cost function is very important in this predictive control algorithm. For the cost function of PTC method, the next-step stator flux $\hat{\psi}_s(k+1)$, rotor flux $\hat{\psi}_r(k+1)$ and the electromagnetic torque $\hat{T}_e(k+1)$ must be calculated. Considering the system state time-delay and parameter uncertainty, the disturbance observer technique is also adopted for improving system robustness. The aim of this section is designing the flux

and current observers. Based on the feedback of stator current information and the stator flux Eq. (1), the stator flux observer is designed as follows:

$$\frac{d}{dt} \hat{\psi}_s = v_s - R_s \cdot i_s + \hat{d}_{\psi_s} + K_{\psi_{sp}} (i_s - \hat{i}_s) \quad (20)$$

$$\hat{d}_{\psi_s} = K_{\psi_{si}} (i_s - \hat{i}_s). \quad (21)$$

Based on Euler discretization method, the discrete time stator flux observer is designed as (22-23);

$$\hat{\psi}_s(k+1) = \hat{\psi}_s(k) + T_s (v_s(k) - R_s \cdot i_s(k) + \hat{d}_{\psi_s}(k) + K_{\psi_{sp}} (i_s(k) - \hat{i}_s(k))) \quad (22)$$

$$\hat{d}_{\psi_s}(k+1) = \hat{d}_{\psi_s}(k) + T_s K_{\psi_{si}} (i_s(k) - \hat{i}_s(k)). \quad (23)$$

Combining the Eqs.(2)-(4), the rotor flux observer is designed as (24-25)

$$\frac{d}{dt} \hat{\psi}_r = \frac{L_m R_r}{L_r} \cdot i_s - \left(\frac{R_r}{L_r} - j \cdot \omega_e \right) \cdot \hat{\psi}_r + K_{\psi_{rp}} (i_s - \hat{i}_s) + \hat{d}_{\psi_r} \quad (24)$$

$$\hat{d}_{\psi_r} = K_{\psi_{ri}} (i_s - \hat{i}_s) \quad (25)$$

the discrete time rotor flux observer is rewritten as;

$$\hat{\psi}_r(k+1) = \hat{\psi}_r(k) + T_s \left(-\left(\frac{R_r}{L_r} - j \cdot \omega_e \right) \cdot \hat{\psi}_r(k) + \frac{L_m R_r}{L_r} \cdot i_s(k) + K_{\psi_{rp}} (i_s(k) - \hat{i}_s(k)) + \hat{d}_{\psi_r}(k) \right) \quad (26)$$

$$\hat{d}_{\psi_r}(k+1) = \hat{d}_{\psi_r}(k) + T_s K_{\psi_{ri}} (i_s(k) - \hat{i}_s(k)). \quad (27)$$

The stator current observer is designed as follows:

$$\begin{aligned} \dot{\hat{i}}_s = & -\frac{T_s L_m^2 R_r}{(L_m^2 - L_r L_s) L_r} i_s + \frac{T_s L_r}{L_m^2 - L_r L_s} R_s i_s \\ & - \frac{T_s L_r}{L_m^2 - L_r L_s} v_s - \frac{T_s L_m}{L_m^2 - L_r L_s} \left(\frac{R_r}{L_r - j\omega} \right) \hat{\psi}_r \\ & \hat{d}_{i_s} + K_{i_{sp}} (i_s - \hat{i}_s) \end{aligned} \quad (28)$$

$$\hat{d}_{i_s} = K_{i_{si}} (i_s - \hat{i}_s) \quad (29)$$

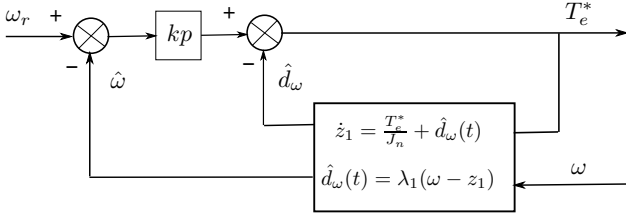


Fig. 3: Torque reference is produced based on disturbance observer.

the discrete time formation of stator current observer is

$$\begin{aligned} \hat{i}_s(k+1) = & (1 - \frac{T_s L_m^2 R_r}{(L_m^2 - L_r L_s) L_r}) \hat{i}_s(k) + \\ & \frac{T_s L_r}{L_m^2 - L_r L_s} R_s \hat{i}_s(k) - \frac{T_s L_r}{L_m^2 - L_r L_s} v_s(k) \\ & - \frac{T_s L_m}{L_m^2 - L_r L_s} (\frac{R_r}{L_r - j\omega}) \hat{\psi}_r(k) \\ & T_s \hat{d}_{i_s}(k) + K_{i_{sp}} T_s (i_s(k) - \hat{i}_s(k)) \end{aligned} \quad (30)$$

$$\hat{d}_{i_s}(k+1) = \hat{d}_{i_s}(k) + T_s K_{i_{si}} (i_s(k) - \hat{i}_s(k)) \quad (31)$$

where T_s is control period.

Define $e_{\psi_s} = \psi_s - \hat{\psi}_s$, $e_{\psi_r} = \psi_r - \hat{\psi}_r$, $e_{i_s} = i_s - \hat{i}_s$, $e_{d_{i_s}} = d_{i_s} - \hat{d}_{i_s}$, $e_{d_{\psi_s}} = d_{\psi_s} - \hat{d}_{\psi_s}$, $e_{d_{\psi_r}} = d_{\psi_r} - \hat{d}_{\psi_r}$, combining Eqs. (20)-(31) and system model, the error system is described as

$$\begin{aligned} \dot{e}_{\psi_s} &= e_{d_{\psi_s}} - K_{\psi_{sp}} e_{i_s} \\ \dot{e}_{d_{\psi_s}} &= \hat{d}_{\psi_s} - K_{\psi_{si}} e_{i_s} \\ \dot{e}_{\psi_r} &= e_{d_{\psi_r}} - (\frac{R_r}{L_r} - j \cdot \omega_e) e_{\psi_r} - K_{\psi_{rp}} e_{i_s} \\ \dot{e}_{d_{\psi_r}} &= \hat{d}_{\psi_r} - K_{\psi_{ri}} e_{i_s} \\ \dot{e}_{i_s} &= e_{d_{i_s}} - \frac{T_s L_m}{L_m^2 - L_r L_s} (\frac{R_r}{L_r - j\omega}) e_{\psi_r} - K_{i_{sp}} e_{i_s} \\ \dot{e}_{d_{i_s}} &= \hat{d}_{i_s} - K_{i_{si}} e_{i_s} \end{aligned} \quad (32)$$

The error system can be described as $\dot{X} = AX + \dot{D}$, so the stability analysis of Eqs. (32) is similar to the above section which also satisfies ISS stability.

C. Predictive Torque Controller Design

The cost function is flexible and can handle system constraints. It should be designed according to the specific control goals. The cost function includes three items: torque error, stator flux error, and over-current protection, i.e.,

$$g_j = \sum_{h=1}^N \{ |T_e^* - \hat{T}_e(k+h)_j| + \lambda (\|\psi_s^*\| - \|\hat{\psi}_s(k+h)_j\|) + I_m(k+h)_j \} \quad (33)$$

The coefficient λ denotes the weighting factor, which weights the relative importance of the electromagnetic torque versus flux control. In the cost function g_j , $h = 2$ is the prediction horizon, j denotes the index of applied voltage vector for the prediction. As a two-level voltage source inverter is applied, there are in total eight different switching states, but seven different voltage vectors. For the PTC method, all switching states must be considered in one sampling interval. In this case $j = 0, \dots, 6$, which means that the cost function must be calculated seven times with one

prediction in order to select the best switching state. The electromagnetic torque reference T_e^* is designed as follows which is calculated by the DOB-based feed forward controller,

$$T_e^* = k_p(\omega_r - \hat{\omega}) - J_n \hat{d}_{\omega} \quad (34)$$

The value of $\hat{T}_e(k+2)_j$ is predicted as follows

$$\hat{T}_e(k+2)_j = \frac{3}{2} \cdot p \cdot \text{Im}(\hat{\psi}_s(k+2) \cdot \hat{i}_s(k+2)) \quad (35)$$

where the the stator current $\hat{i}_s(k+2)$ and $\hat{\psi}_s(k+2)$ can be predicted based on the Eqs.(20)-(31).

The over-current protection is activated when the absolute value of the predicted current is higher than its limit. The current limitation is defined as

$$I_m(k+2) = \{0, \text{if } |i(k+2)| \leq |i_{max}|, r \gg 0\} \quad (36)$$

If the current $i(k+2)$ beyond the limit, the cost function will make the voltage vector will not be chosen. This seems to prevent the control of the motor if the current becomes greater than i_{max} , but the safety of the control system is guaranteed which is one of the important advantage than other control methods.

Remark 3.1. For the cost function of PTC control, the accuracy and generating rate of torque reference is more important for the system control performance. The existed torque reference signal which is generated by PI controller, it is not a good solution especially when the load torque is given and the system exist other parameter uncertainty. From natural consideration, if the load torque and parameter uncertainty is measured, then the torque reference is produced as soon as possible. The proposed disturbance observer technique is motivated by this idea, similar to the soft measurement methods, the DOB method can estimate the load torque, other parameter uncertainty and the convergence rate is ensured by tuning the observer parameters. In addition, the DOB technique is also extended for the flux and current observer design, it can improve the system robustness.

IV. SIMULATION AND EXPERIMENTAL STUDIES

In what follows, the performances of the proposed disturbance observer based PTC method (DOB-PTC) is illustrated via numerical simulations and experimental verification. The induction motor parameters in this test are shown in Table 1.

Table 1: Parameter Values of Induction motor

Descriptions	Parameters	Nominal Values
DC link Voltage	V_{dc}	582 (V)
Stator Resistance	R_s	2.68 Ω
Rotor Resistance	R_r	2.13 Ω
Inductance	L_m	275.1 (mH)
Stator Inductance	L_s	283.4 (mH)
Rotor Inductance	L_r	283.4 (mH)
Pole Pairs	P	1.0
Speed	ω_{nom}	2772.0 (RPM)
Torque	T_{nom}	7.5 (Nm)
Inertia	J	0.005 Kg \cdot m ²

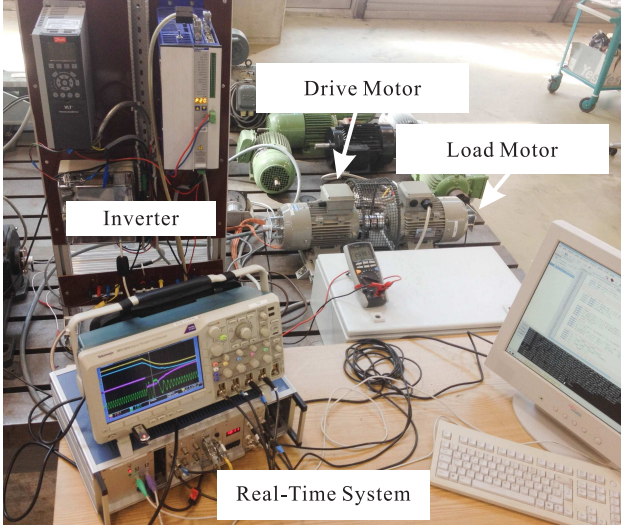


Fig. 4: Test bench description.

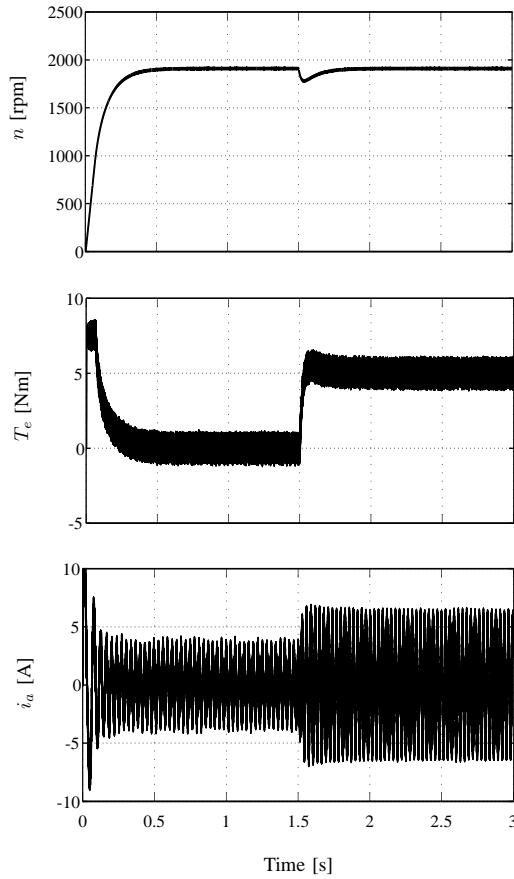


Fig. 5: Speed, torque, stator current waveforms when the rated speed is $\omega_r = 1910$ rpm and the torque is given at 5 Nm.

A. Simulation Studies

A simulation comparison in a MATLAB/Simulink environment is performed. The parameters of the main motor are given in Table 1. They are obtained from the machine tested in the laboratory. The sample frequency is set at 16 kHz, which is the same to the test experimental setup in 4. The desired speed is set to be $\omega_r = 1910$ rpm.

In order to show the advantages of the novel disturbance

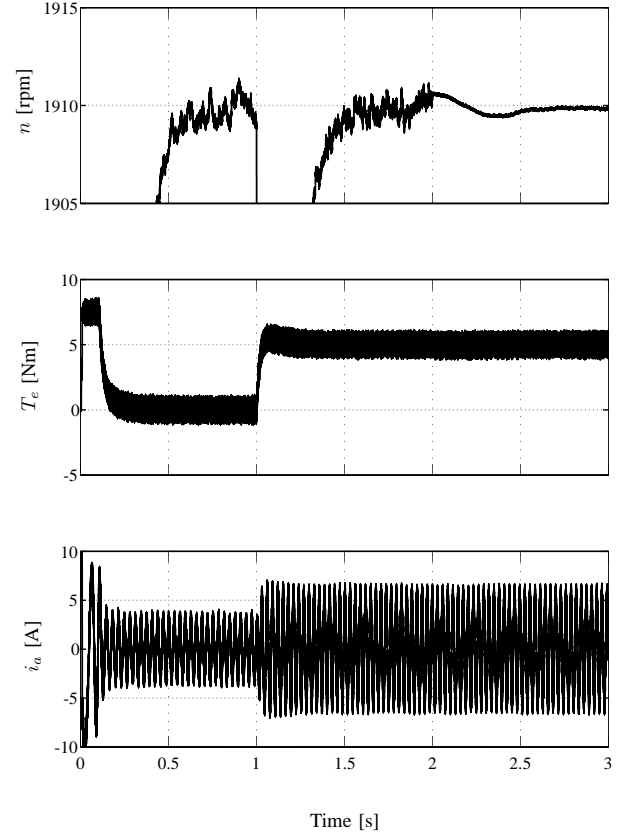


Fig. 6: Speed, torque, stator current waveforms when the rated speed is $\omega_r = 1910$ rpm and the inertia value is given at $20 J_{nom}$.

observer based predictive torque control method proposed in this paper, the induction motor is numerically simulated using the simulation model, we will use simulations to verify the performance based on the induction motor system with torque load disturbance and inertia value varying.

First, to verify the disturbance rejection ability of the proposed DOB-PTC method, load torque variation is considered, simulation is also carried out for it. The parameters in DOB-PTC controller are selected as $k_p = 0.06$, $\lambda = 18$, $\lambda_1 = 100$. From Fig. 5, we can find that the speed response is also good when the load torque is given at $T_L = 5$ Nm.

In addition, for verifying the robustness of the proposed method, the inertia value is also varying, from Fig. 6, we can find that the robustness of closed loop performance is insured even if the inertia value is changed at $20J_{nom}$.

B. Experimental Studies

The proposed DOB-PTC method has been verified on an experimental test bench. It consist of two 2.2 Kw squirrel-cage IMs. One motor is used as a load machine which is driven by a Danfoss VLT FC 302 3.0 kW inverter. The main machine is driven by a modified SERVOSTAR620 14-kVA inverter, which provides full control of the insulated-gate bipolar transistor gates. A self-made 1.4 GHz real-time computer system is used. The rotor position is measured by a 1024-point incremental encoder. The parameters of the

induction motor are given as Table 1. Fig. 4 shows a picture of the test bench. Some experimental result description is compared with traditional PTC method which is proposed in [16].

The test is to verify the system performance during a rated speed reverse maneuver. The speed reference changes from 2772 rpm to -2772 rpm and then returns to 2772 rpm. The speed response, the electromagnetic torque and the stator current are presented in Fig. 7. The recorded average switching frequency is 3.0 kHz. During the dynamic response process, the electromagnetic torque reaches its saturation value 7.5 Nm for the shortest settling time. Fig. 9 presents the stator flux in α, β frame and its magnitude value during the dynamic process of the speed reverse maneuver. The reference value of stator flux magnitude is 0.71 Wb. The picture shows that the accurate flux response (the ripple is less than 0.05 Wb) are achieved in the whole range. The reason is that the flux is considered in the design of cost function.

Figs. 8-10 show that speed steady response and the torque as well as the current behaviors are acceptable. Especially in Fig. 8, we can conclude that the system disturbance reject ability is also ensured when the load torque is given. The torque ripple is about 0.6 Nm when the load torque is given at 3.75 Nm. The flux in Fig. 9 can also be accepted. When the system is given at full load in Fig. 10, the torque ripple is about 1.0 Nm, which is better than traditional PTC method in [16], the steady torque accuracy is improved. Thus, the disturbance observer and PTC method are completely coordinated.

To verify the torque dynamics clearly, a test has done for showing the torque step performance. In Fig. 11, The experiment tests the system performance with a full load impact at the rated speed (2772 rpm). A sudden load change (from no load to 7.5 Nm) is given at 0.48s. The speed recovery process only need 0.42s which is also faster than traditional PTC method.

The torque reference is generated by proposed controller, alters from zero to the rated value (7.5 Nm), torque reference and torque response are compared. Fig. 12 shows that the system is stable over a full load disturbance. It must be noticed that the injected load torque (generated by a commercial inverter) is not a step response, which is the reason that the torque response looks slower than the described. From Fig. 12, the torque ripple is less than 1.0 Nm and the settling time is around 370 μ s. This fast torque response and low torque precision is one of the advantage for this DOB-PTC control method.

From 13-14, when the inertia value J and R_s is varying, the system is also stable until the initial value linearly increased to 2000% of the original value, that is to say ($J = 20J_{nom} = 0.1 \text{ Kg} \cdot \text{m}^2$) and R_s which is linearly increased to the original value of 192%, it is better than PTC method which is 160% of original value. The system robustness is improved by the proposed control method. From the above experimental results, compared with the traditional PTC method for induction motor system which described in [16], we can conclude that not only the load torque disturbance reject ability, but also the system robustness is improved obviously by the proposed DOB-PTC method. The system dynamic response and steady state performance

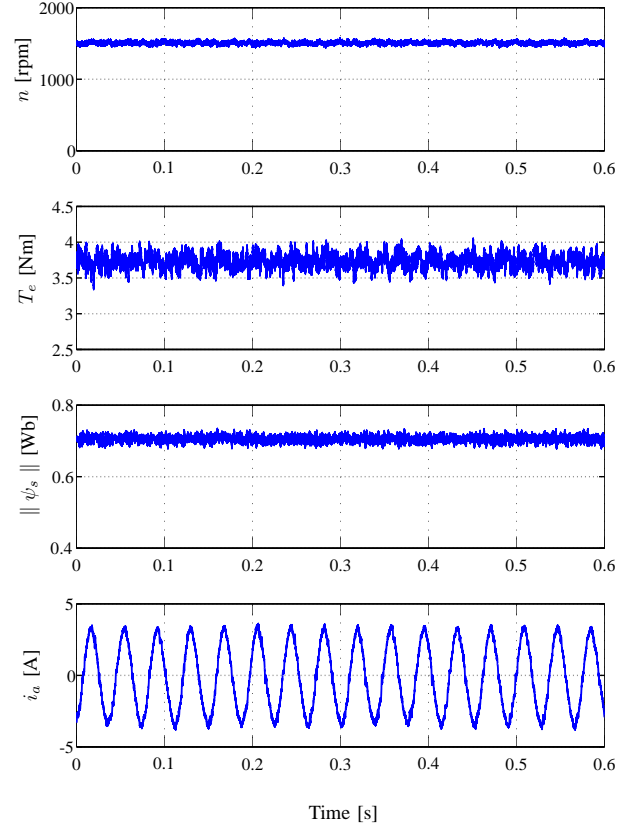


Fig. 8: Steady state performance: speed, torque, stator flux and stator current waveforms when the rated speed is 1500 rpm and the torque is given at 3.75 Nm.

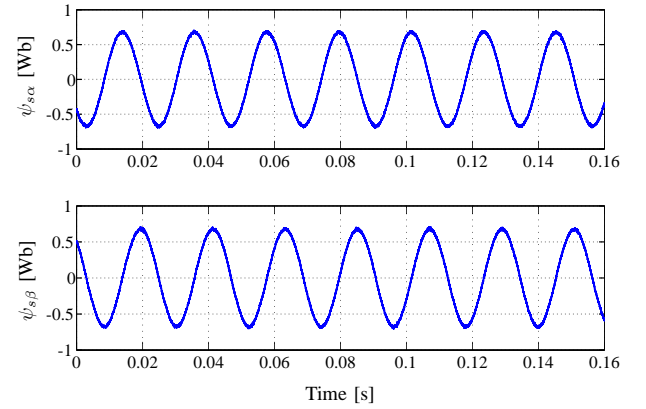


Fig. 9: Steady state performance: stator flux waveforms.

is also ensured. That is to say, disturbance observer based predictive control method can improve system robustness and disturbance reject ability which not sacrificing the nominal performance.

V. CONCLUSION

The novel disturbance observer based robust predictive torque control method for the induction system has been studied in this paper. By utilizing the disturbance estimation technique based on disturbance observers, a novel predictive torque controller has been developed. The PTC method may

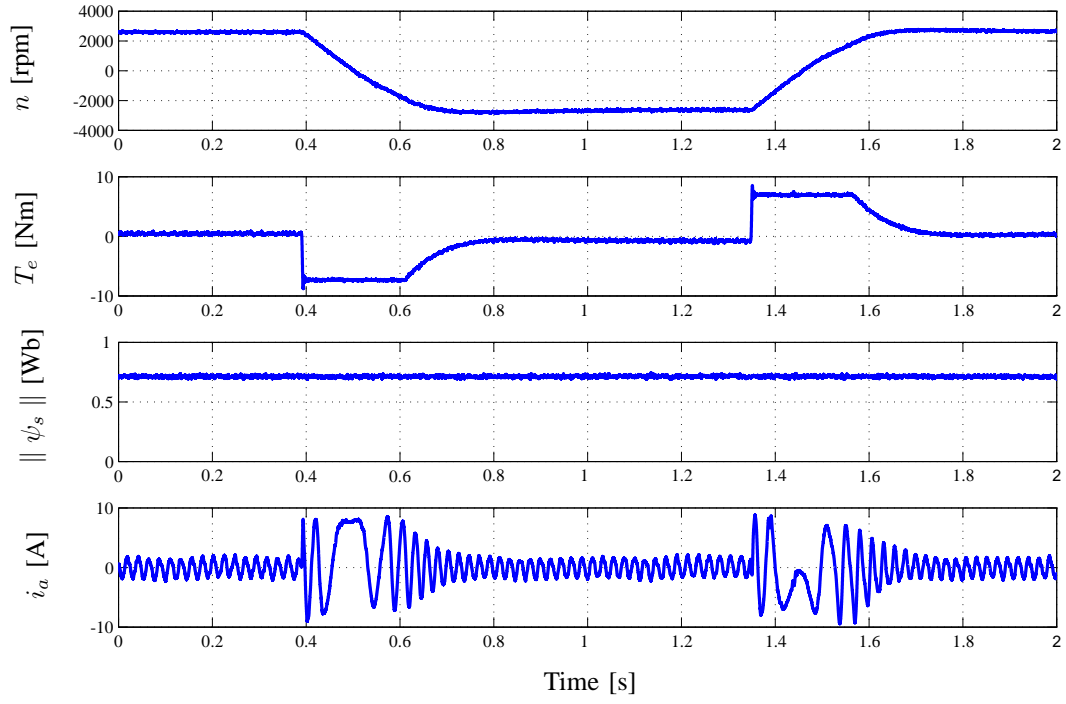


Fig. 7: Speed, torque, stator flux and stator current waveforms during the rated full speed reversal process (2772 rpm to -2772 rpm).

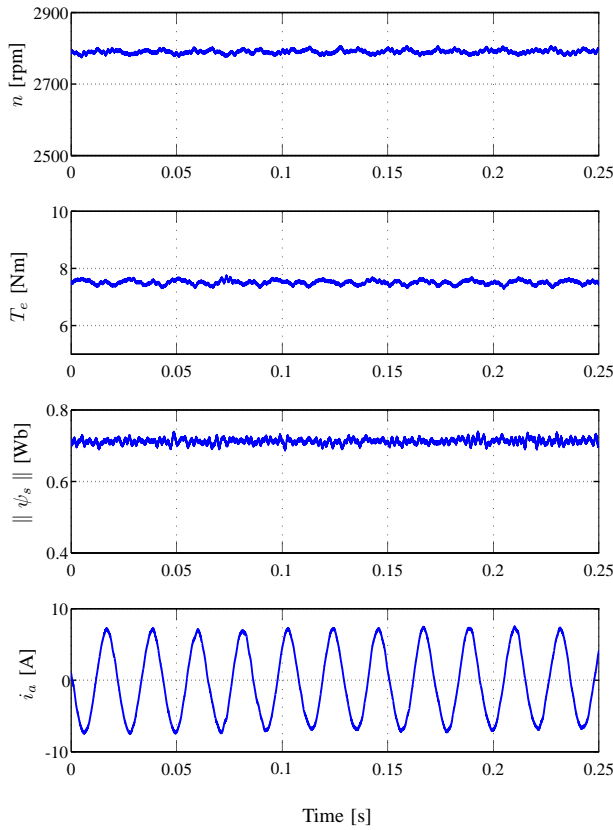


Fig. 10: Steady state performance: speed, torque, stator flux and stator current waveforms when the rated speed is 2772 rpm and the torque is given at 7.5 Nm.

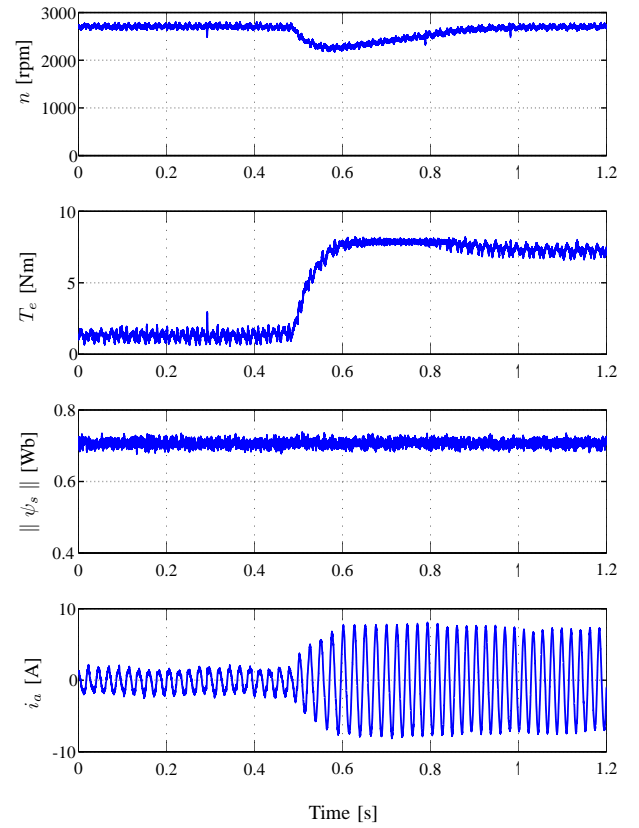


Fig. 11: Dynamic response: speed, torque, stator flux and stator current waveforms when the rated speed is 2772 rpm and the torque is given at 7.5 Nm.

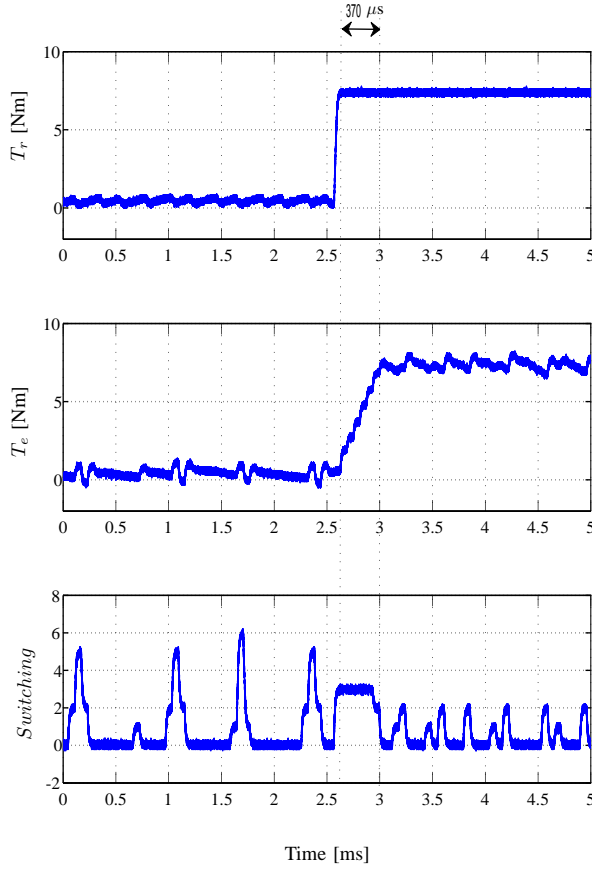


Fig. 12: Dynamic response: torque reference, torque and switching signal.

be further simple and more easy to be implemented. In addition, the robustness and disturbance reject ability is improved by the proposed design. The system ability analysis is also given. The simulation and experimental results for the controller show that it not only makes the states of closed loop system obtain better tracking performance, but also provides a better disturbance rejection ability against torque load disturbance and parameter variation.

REFERENCES

- [1] I. Takahashi and T. Noguchi, "A new quick-response and high efficiency control strategy of an induction machine," *Industrial Application, IEEE Transactions on*, vol. IA-22, no. 22, pp. 820-827, 1986.
- [2] T. G. Habetler, F. Profumo, M. Pastorelli, and L. M. Tolbert, "Direct torque control of induction machines using space vector modulation," *Industrial Application IEEE Transactions on*, vol. 28, no. 5, pp. 1045-1054, 1992.
- [3] J. K. Kang and S. K. Sul, "New direct torque control of induction motor for minimum torque ripple and constant switching frequency," *Industrial Application, IEEE Transactions on*, vol. 35, no. 5, pp. 1076-1072, 1999.
- [4] V. Ambrozic, G. Buja, and R. Menis, "Band-constrained technique for direct torque control of induction motor," *Industrial Electronics, IEEE Transactions on*, vol. 51, no. 4, pp. 776-784, 2004.
- [5] G. S. Buja and M. P. Kazmierkowski, "Direct torque control of PWM inverter-fed AC motors-A survey," *Industrial Electronics, IEEE Transactions on*, vol. 51, no. 4, pp. 744-757, 2004.
- [6] C. Lascu, I. Boldea, and F. Blaabjerg, "Variable-structure direct torque control: A class of fast and robust controllers for induction machine drives," *Industrial Electronics, IEEE Transactions on*, vol. 51, no. 4, pp. 785-792, 2004.
- [7] C. Lascu, I. Boldea, and F. Blaabjerg, "Direct torque control of sensorless induction motor drives: A sliding-mode approach," *Industrial Electronics, IEEE Transactions on*, vol. 40, no. 2, pp. 582-590, 2004.

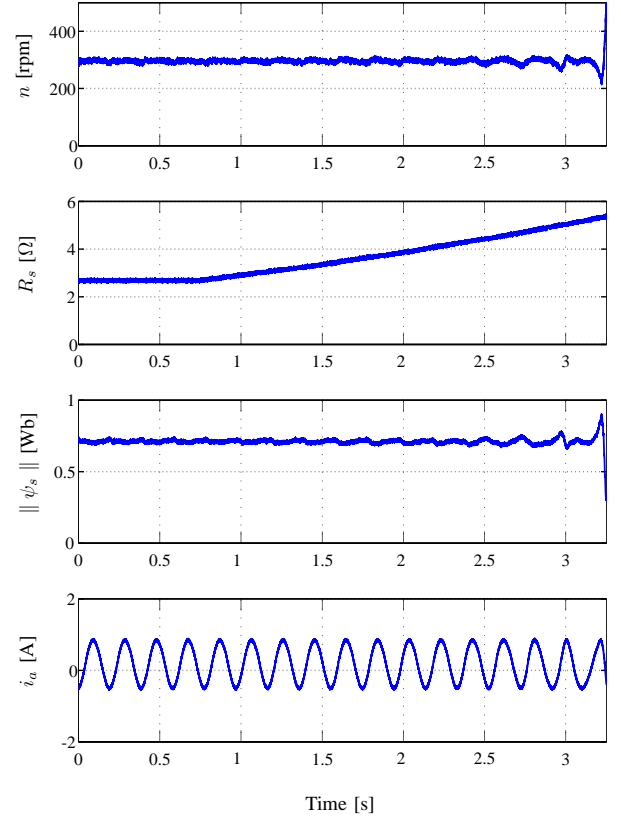


Fig. 13: Robustness: speed (the rated speed is 300 rpm), stator resistance, stator flux, stator current waveforms when the stator resistance is varying.

- [8] P. Correa, M. Pacas, and J. Rodriguez, "Predictive torque control for inverter-fed induction machines," *Industrial Electronics, IEEE Transactions on*, vol. 54, no. 2, pp. 1073-1079, 2007.
- [9] P. Cortes, P. Kazmierkowski, R. M. Kennel, D. E. Quevedo, and J. Rodriguez, "Predictive control in power electronics and drives," *Industrial Electronics, IEEE Transactions on*, vol. 55, no. 12, pp. 4312-4324, 2008.
- [10] M. Nemec, D. Nedeljkovic, and V. Ambrozic, "Predictive torque control of induction machines using immediate flux control," *Industrial Electronics, IEEE Transactions on*, vol. 54, no. 4, pp. 2009-2017, 2007.
- [11] R. Vargas, U. Ammann, B. Hudofsky, and J. Rodriguez, "Predictive torque control of an induction machine fed by a matrix converter with reactive input power control," *Power Electronics, IEEE Transactions on*, vol. 25, no. 6, pp. 1426-1438, (2010).
- [12] S. A. Davari, D. A. Khaburi, F. Wang, et al. "Using full order and reduced order observers for robust sensorless predictive torque control of induction motors," *Power Electronics, IEEE Transactions on*, vol. 27, no.7, pp. 3424-3433, (2012).
- [13] T. Geyer, G. Papafotiou, M. Morari. "Model predictive direct torque control-part I: concept, algorithm, and analysis," *Industrial Electronics, IEEE Transactions on*, vol. 56, no. 6, pp. 1894-1905, 2009.
- [14] T. Geyer. "Model predictive direct torque control: derivation and analysis of the state-feedback control law," *Industry Applications, IEEE Transactions on*, vol. 49, no.5, pp. 2146-2157, 2013.
- [15] J. Scoltock, T. Geyer, U. K. Madawala. "A comparison of model predictive control schemes for MV induction motor drives," *Industrial Informatics, IEEE Transactions on*, vol. 9, no. 2, pp. 909-919, 2013.
- [16] F. Wang, S. Li, X. Mei, et al. "Model based predictive direct control strategies for electrical drives: an experimental evaluation of PTC and PCC Methods," *Industrial Informatics, IEEE Transactions on*, vol. 11, no.3, pp. 671-681, 2015.
- [17] J. Holtz and J. Quan, "Drift and parameter compensated flux estimator for persistent zero stator frequency operation of sensorless controlled induction motors," *Industrial Application, IEEE Transactions on*, vol. 39, no. 4, pp. 1052-1060, 2003.

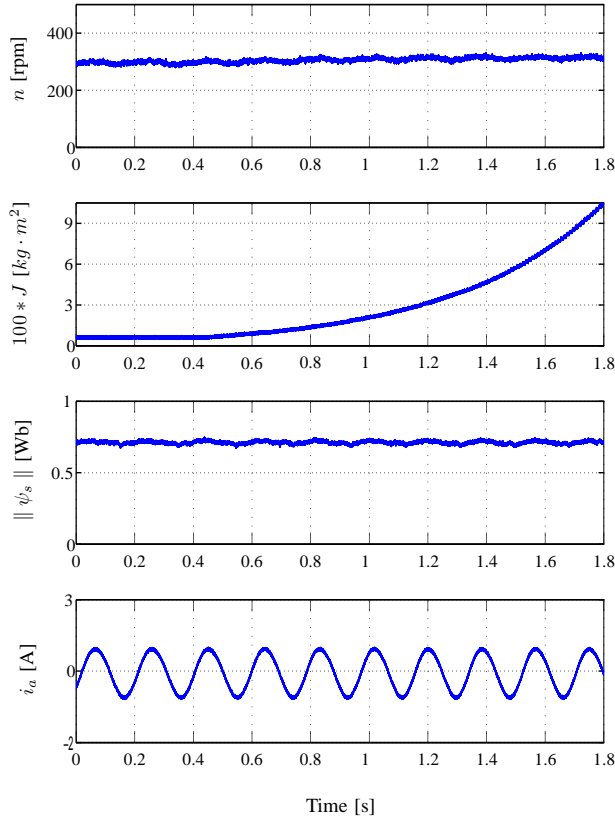


Fig. 14: Robustness: speed (the rated speed is 300 rpm), inertia, stator flux and stator current waveforms when the inertia value is varying.

[18] J. Holz. "Sensorless Control of induction machines with or without signal injections," *Industrial Electronics, IEEE Transactions on*, vol. 53, no.1, pp. 7-30, 2006.

[19] S. Kwak, U. C. Moon, and J. C. Park. "Predictive control based direct power control with an adaptive parameter identification technique for improved AFE performance," *Power Electronics, IEEE Transactions on*, vol. 29, no.11, pp. 6178-6187, 2014.

[20] J. Rodriguez, J. Pontt, C. A. Silva, P. Correa, P. Lezana, P. Cortes, and U. Ammann. "Predictive current control of a voltage source inverter," *Industrial Electronics, IEEE Transactions on*, vol. 54, no.1, pp. 495-503, 2007.

[21] H. Young, M. Perez, J. Rodriguez. "Analysis of finite-control-set model predictive current control with model parameter mismatch in a three-phase inverter," *Industrial Electronics, IEEE Transactions on*, online, 2015.

[22] J. Rodriguez, P. Cortes. "Predictive control of power converters and electrical drives," *1st ed. Wiley-IEEE Press*, 2012.

[23] Z. Xu and M. Rahman, "Comparison of a sliding observer and a kalman filter for direct-torque-controlled IPM synchronous motor drives," *Industrial Electronics, IEEE Transactions on*, vol. 59, no. 11, pp. 4179-4188, 2012.

[24] C. Schauder, "Adaptive speed identification for vector control of induction motors without rotational transducers," *Industry Applications, IEEE Transactions on*, vol. 28, no. 5, pp. 1054-1061, 1992.

[25] K. S. Low and H. Zhuang, "Robust model predictive control and observer for direct drive applications," *Power Electronics, IEEE Transactions on*, vol. 15, no. 6, pp. 1018-1028, 2000.

[26] M. J. Youn. "A nonlinear speed control for a PM synchronous motor using a simple disturbance estimation technique," *Industrial Electronics, IEEE Transactions on*, vol. 49, no. 3, pp. 524-535, 2002.

[27] J. Han, "From PID to active disturbance rejection control," *IEEE Trans. Ind. Electron.*, vol. 56, no. 3, pp. 900-906, 2009.

[28] S. H. Li and Z. G. Liu. "Adaptive speed control for permanent-magnet synchronous motor system with variations of load inertia," *Industrial Electronics, IEEE Transactions on*, vol. 56, no. 8, pp. 3050-3059, 2009.

[29] H. X. Liu, S. H. Li. "Speed control for PMSM servo system using predictive functional control and extended state observer," *Industrial Electronics, IEEE Transactions on*, vol. 59, no. 2, pp. 1171-1183, 2012.

[30] W. H. Chen, "Disturbance observer based control for nonlinear systems," *Mechatronics, IEEE/ASME Transactions on*, vol. 9, no. 4, pp. 706C710, Dec. 2004.

[31] S. H. Li, J. Yang, W. H. Chen, X. S. Chen. *Disturbance observer-based control: methods and applications*, CRC press, 2014.

[32] B. Sun and Z. Gao, "A DSP-based active disturbance rejection control design for a 1-kW H-bridge DC-DC power converter," *Industrial Electronics, IEEE Transactions on*, vol. 52, no. 5, pp. 1271-1277, 2005.

[33] M. Nakao, K. Ohnishi, and K. A. Miyachi. "Robust decentralized joint control based on interference estimation," *IEEE International Conference on Robotics and Automation*, vol. 4, pp. 326-331, 1987.

[34] L. Guo, and W. H. Chen. "Disturbance attenuation and rejection for systems with nonlinearity via DOBC approach," *International Journal of Robust Nonlinear Control*, vol. 15, no. 3, pp. 109-125, 2005.

[35] F. Castanos, and L. Fridman. "Analysis and design of integral sliding manifolds for systems with unmatched perturbations," *Automatic Control, IEEE Transactions on*, vol. 51, no. 5, pp. 853-858, 2006.

[36] H. K. Khalil. *Nonlinear Systems*, 3rd ed. Upper Saddle River, NJ, USA: Prentice-Hall, 2002.